Scientia Iranica F (2016) 23(3), 1517–1523

Sharif University of Technology
Scientia Iranica
Transactions F: Nanotechnology
www.scientiairanica.com

The effect of catalyst combination ratio on growth of carbon nanotubes over Fe-Co/nanometric SiC by chemical vapor deposition

F. Shahi and M. Akbarzadeh Pasha*

Department of Solid State Physics, University of Mazandaran, Babolsar, P.O. Box 47416-95447, Iran.

Received 12 April 2015; received in revised form 17 February 2016; accepted 9 April 2016

KEYWORDS
CNTs;
CVD;
Bimetallic catalyst;
SiC;
Combination ratio.

Abstract. Bimetallic Fe-Co catalysts supported on nanometric SiC powder were prepared by wet impregnation method and were used to catalyze CNTs from decomposition of acetylene at 850°C by TCVD. The effect of Fe and Co combination ratio in catalytic basis on properties of the end product CNTs was investigated using XRD, SEM, TEM, and Raman spectroscopy. The results revealed that iron and cobalt were in oxide and cobalt ferrite forms. The best growth of CNTs in the catalyst sample with wt% Fe:Co:SiC=10:10:80 was achieved. It was observed that the ratio of Fe:Co loading in catalyst-substrate composition was an important factor which could affect the activity of catalytic basis and the characteristics of grown CNTs, such as the density and average diameter.

1. Introduction

Carbon nanotubes (CNTs) are seamless coaxial cylinders of one or more graphene layers (denoted by single wall, SWCNT, or multiwall, MWCNT) with open or closed ends. The techniques widely used for the synthesis of CNTs [1,2] are arc discharge [3-5], laser ablation [6,7], and Chemical Vapor Deposition (CVD) [8-11]. Nowadays, CVD is the most popular method of producing CNTs [12]. In this method, thermal decomposition of a hydrocarbon vapor is achieved in the presence of a metal catalyst often supported on a substrate. The CNTs have wide applications in the fields of condensed matter physics and nanophase materials due to their nanometer-sized tubular structure and the excellent physical, chemical, optical, and magnetic properties [13-15]. Due to its wide-band gap semi-conducting feature, silicon carbide (SiC) may find extensive applications for high-temperature, high-frequency, and high-power electronics. The combination of SiC and CNTs may create some new features for their future applications in electronic devices [16]. Murakami et al. have reported growth of SWCNTs on SiC by CVD using ethanol as a carbon source [17]. Also, MWCNTs were grown on the surface of oxidized SiC whiskers by a xylene-ferrocene (carbon source-catalyst source) CVD process [16].

This paper aims to grow CNTs on a bimetallic catalyst (Fe-Co) supported on nanometric SiC substrate by Thermal Chemical Vapor Deposition (TCVD). We investigate the effect of Fe and Co combination ratio in bimetallic catalyst basis on properties of the end product CNTs.

2. Material and methods

In this research, the starting materials were silicon carbide nanopowder (SiC, Beta, 99+ %) with an average size of 45-65 nm (US Research Nanomateri-

*. *Corresponding author. Tel:+98 11 35302480; Fax: +98 11 35302480*
E-mail address: m.akbarzadeh@umz.ac.ir (M. Akbarzadeh Pasha)

Table 1. Designations of different catalyst samples based on their composition ratio.

Catalyst designation	Fe:Co:SiC
C1	20:0:80
C2	15:5:80
C3	10:10:80
C4	5:15:80
C5	0:20:80

als, Inc.), $Fe(NO_3)_3.9H_2O$ (supplied by Merck), and $Co(NO_3)_2.6H_2O$ (supplied by Merck). Bimetallic catalysts with different wt% proportions of Fe:Co:SiC = 20:0:80, 15:5:80, 10:10:80, 5:15:80, and 0:20:80 were prepared using wet impregnation method. Table 1 shows the designation of different catalyst samples (based on composition ratio) prepared in the present work. 1 g SiC powder was dispersed in 20 ml of ethanol and stirred (∼800 rpm) for 20 min in order to obtain a homogeneous suspension. Appropriate stoichiometric amounts of $Fe(NO_3)_3.9H_2O$ (1.81, 1.37, 0.94, 0.43, and 0 gram for C1, C2, C3, C4, and C5, respectively) and $Co(NO_3)_2.6H_2O$ (0, 0.30, 0.64, 0.94, and 1.23 gram for C1, C2, C3, C4, and C5, respectively) were solved in 5 ml distilled water, separately, and then were gradually added to the SiC suspension. The final mixture after 30 min of stirring was dried at 80°C and calcinated at 800°C under air atmosphere for 2 h and catalyst basis was obtained.

The synthesis of CNTs was carried out by a TCVD system using a horizontal tubular quartz reactor at atmospheric pressure. The precursor gas was composed of acetylene and argon (C_2H_2/Ar = 15/150 Sccm) flows over the catalyst at 850°C for 15 minutes. After CNT synthesis, the reactor was cooled down and the product (carbon deposit) formed along with the catalyst was weighed and characterized.

X-Ray Diffraction (XRD) patterns of the catalyst powders were prepared using GBC diffractometer (Cu kα, λ = 1.5406 Å). The morphology and structure of CNTs were observed using Field Emission Scanning Electron Microscopy (FE-SEM, MIRA TESCAN, accelerating voltage of 15 kV) and Transmission Electron Microscopy (TEM, Zeiss - EM10C microscope working at 80 KV). Raman spectra of grown CNTs were recorded with Dispersive Raman Microscope SENTERRA BRUKER using a laser wavelength of 785 nm.

3. Results and discussion

The XRD patterns of the five different Fe-Co loaded catalysts supported on nanometric SiC are shown in Figure 1. The silicon carbide has the β-SiC crystal structure. X-ray diffraction of C2 and C3 samples (Figure 1(b) and (c)) shows the formation of cobalt ferrite ($CoFe_2O_4$) nanoparticles. It can be seen that

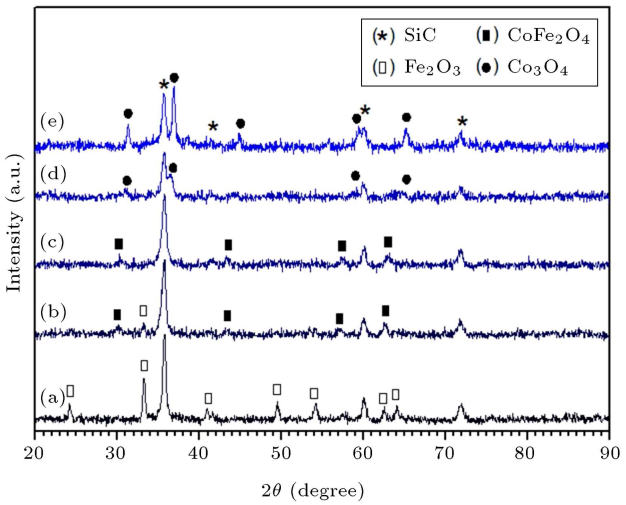

Figure 1. XRD patterns of (a) C1, (b) C2, (c) C3, (d) C4, and (e) C5 catalytic bases.

increasing the cobalt wt% in C2 and C3 catalysts elevates the intensity of $CoFe_2O_4$ peaks, which is an evidence of increase in the amount of nanoparticles. In C4 catalyst (Figure 1(d)), iron oxide has not been detected, probably because of its small amount. The approximate size of catalytic nanoparticles was determined from the X-ray diffraction peak broadening using the Scherrer formula [18]:

$$D = \frac{K\lambda}{\beta \cos\theta}, \tag{1}$$

where D is the crystallite size, K is the shape factor (0.89), λ is the X-ray wavelength (1.5406 Å), β is the peak broadening at half maximum (Full Width at Half Maximum: FWHM), and θ is the diffraction angle.

The approximate sizes of catalytic nanoparticles along with their standard deviations are given in Table 2. (It seems that the catalytic nanoparticles have rather spherical shapes, thus, roughly speaking, the reported sizes of catalytic particles can be identified

Table 2. The approximate sizes of catalytic nanoparticles along with their standard deviations prepared on different catalyst samples.

Catalyst	Metal oxide	Approximate size of particle (nm)	Standard deviation of particle size (nm)
C1	Fe_2O_3	26.3	4.5
C2	Fe_2O_3	27.7	4.5
	$CoFe_2O_4$	16.2	2.5
C3	$CoFe_2O_4$	14.0	3.6
C4	Co_3O_4	17.4	4.7
C5	Co_3O_4	23.6	6.1

as their diameter.) The minimum size of catalytic nanoparticles has been achieved at C3 catalyst sample. The carbon yield percentage of catalytic basis is calculated by the following equation:

$$\text{Carbon yield}(\%) = \frac{M_{\text{Total}} - M_{\text{Cat}}}{M_{\text{Cat}}} \times 100, \qquad (2)$$

where M_{Total} is the total mass of final product (catalyst + carbon deposit) and M_{Cat} is the initial mass of catalyst. Figure 2 shows the carbon yield percentage of the prepared catalysts as a function of Fe:Co loading. Considering Fe:Co ratio, by increasing the contribution of Co, the carbon yield is first constant (till the %wt of Co reaches that of Fe; Fe:Co $\geq$ 10:10) and then decreases (when %wt of Co exceeds that of Fe; Fe:Co<10:10).

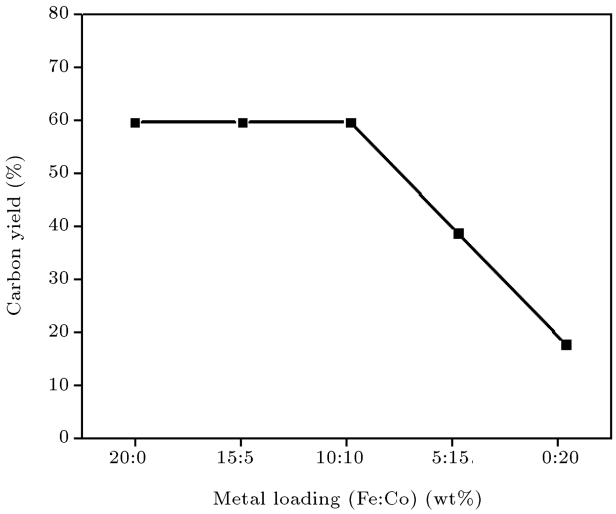

Figure 2. Metal loading dependence of carbon yield of catalyst samples.

Figure 3 shows the representative FE-SEM images of grown CNTs on different (a) C1, (b) C2, (c) C3, (d) C4, and (e) C5 catalyst samples. Successful growth of CNTs on almost all types of prepared catalysts confirms that nanometric SiC powder can be applied as an appropriate support in the CVD growth of CNTs. It is obvious that the density of grown CNTs dramatically decreases when Co concentration exceeds that of Fe in catalyst composition (samples C4 and C5). On SiC support, pure Co catalyst shows very weak activity for catalyzing CNT synthesis compared to pure Fe. Moreover, the activity of iron appears to be strongly affected by mixing it with cobalt. Histograms of diameter distribution of grown CNTs, fitted with normal curves, are shown in Figure 4. The average diameter of CNTs, along with their standard deviations, obtained on different catalysts is reported in Table 3. Increasing the weight percent of Co strongly reduces the diameters of originated CNTs till the Co content exceeds that of Fe. When Fe:Co ratio is 10:10 (sample C3), the diameter of CNTs gets its minimum value and the distribution of diameters achieves nearly maximum uniformity. After this criti-

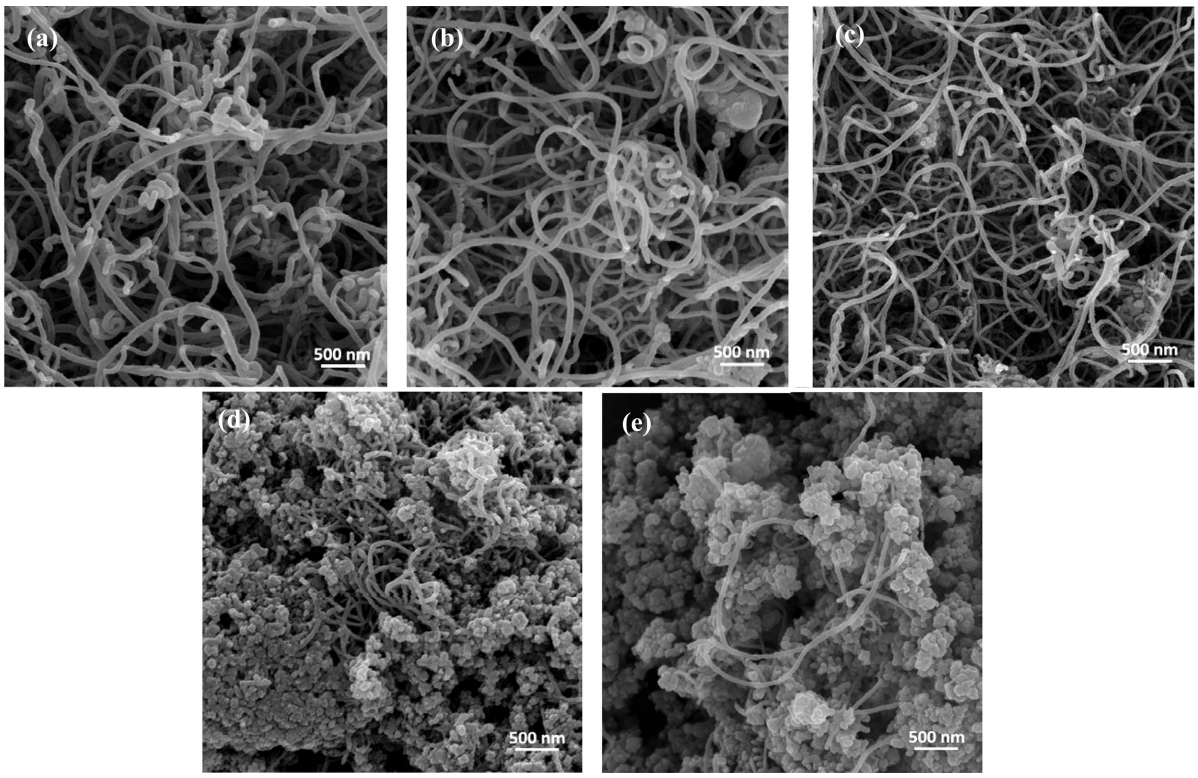

Figure 3. SEM micrographs of the grown CNTs on (a) C1, (b) C2, (c) C3, (d) C4, and (e) C5 catalyst samples.

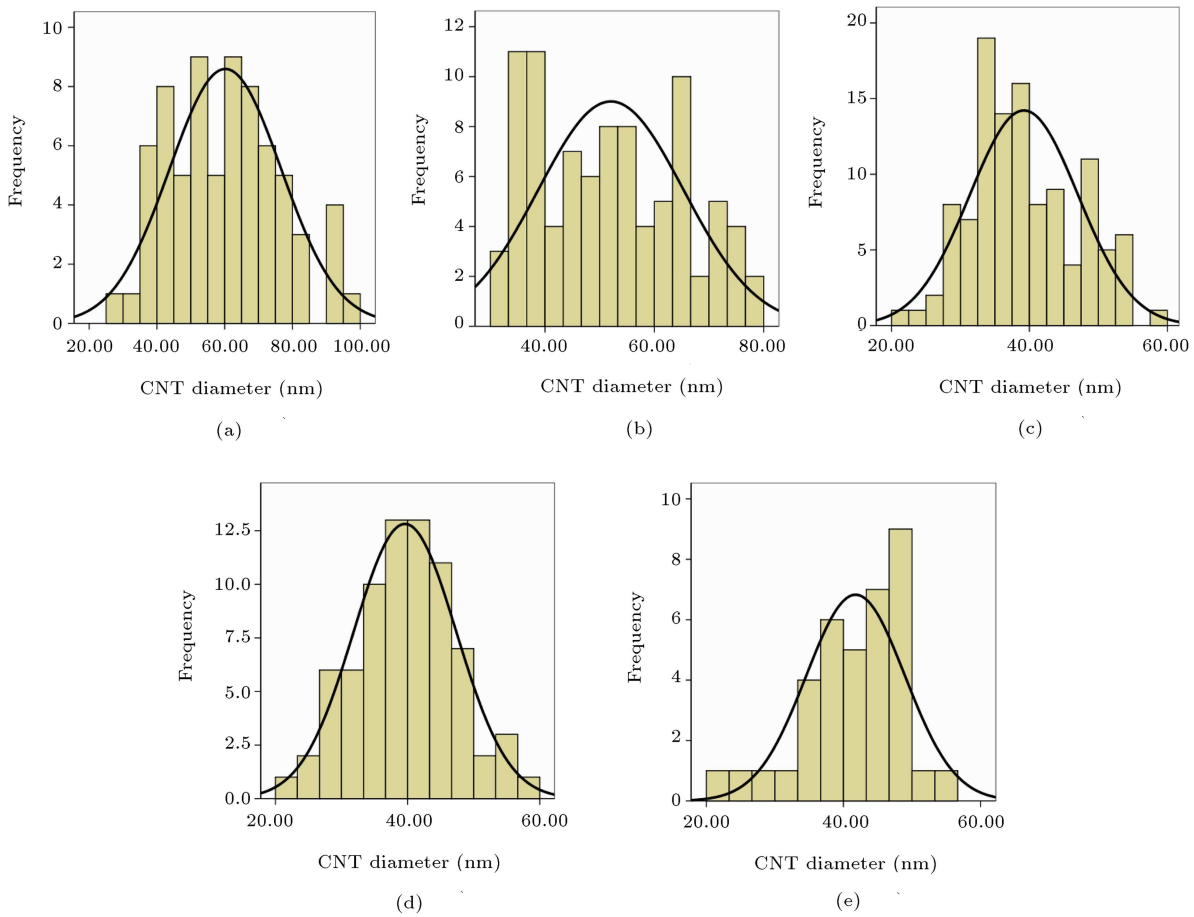

Figure 4. Diameter distribution histograms (fitted with normal curves) of grown CNTs on (a) C1, (b) C2, (c) C3, (d) C4, and (e) C5 catalyst samples.

Table 3. Average diameters of grown CNTs and their standard deviations on different catalyst samples.

Catalyst	Average diameter of CNTs (nm)	Standard deviation of average diameter (nm)
C1	60.2	16.5
C2	52.1	13.3
C3	39.2	7.9
C4	39.9	7.5
C5	41.8	7.2

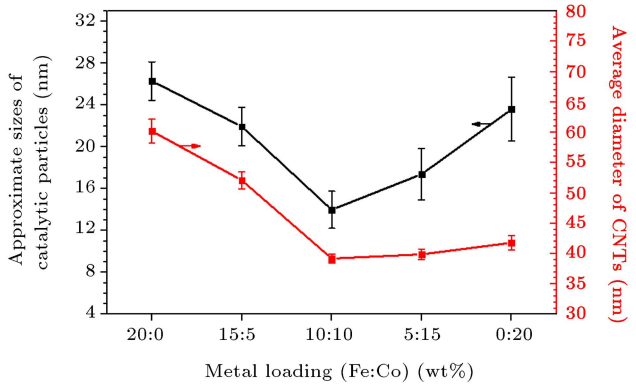

Figure 5. Dependence of catalytic particle sizes and CNTs' average diameters on metal loading.

cal ratio, increasing Co content gradually raises CNT diameter. As we expected, this result is in agreement with the previous finding for catalytic particle sizes (Table 2).

Figure 5 shows that the dependence of CNTs' average diameter and that of catalyst particle size on Fe:Co loading ratio (for C2 catalyst sample, the mean value of 16.2 and 27.7 nm was chosen as particle sizes) are similar, which supports the fact that there is a strong correlation between catalyst particle size and CNT diameter (error bars in Figure 5 indicate the Standard Errors (SE) which are related to Standard Deviations (SD) of the reported data via the relation SE=SD/$\sqrt{n}$, where n is the size of statistical sample). Considering SEM observation beside carbon yield result, we can conclude that the best catalyst composition for CNT production is C3 catalyst sample, Fe:Co:SiC=10:10:80. It seems that the presence of $CoFe_2O_4$ in this sample increases its catalytic activity and improves its efficiency for CNT production. Also,

it was observed that iron oxide nanoparticles show higher efficiency than cobalt oxide particles for CNT production on nanometric SiC support. Similar result has been reported by other researchers [19]. Klinke et al. tested Fe-, Co-, and Ni-based catalysts on silica to grow CNTs from acetylene. They observed that iron produces the highest density of carbon structures at any considered temperature in the range of 580-1000°C [20]. Hernadi et al. tested Fe- and Co-based catalysts on various supports and different hydrocarbons as carbon sources. They observed that iron/silica presents the maximum activity for decomposition of different unsaturated compounds [21]. Another group of researchers concluded that Fe is more active than Co, but the quality (graphitization and structure) of the grown CNTs is better with Co [19].

Figure 6 shows the TEM images of CNTs synthesized on C3 catalyst sample with wt% Fe:Co:SiC = 10:10:80. Generally, it reveals the hollow core and tubular structure of the grown carbon products, which confirms that the filamentous morphologies seen in SEM observation are carbon nanotubes and not carbon fibers. The synthesized CNTs have often straight or curved structures (Figure 6(a)); however, some helix nanotubes can be observed in the final carbon deposit as indicated with red arrow in Figure 6(b). TEM observation revealed that the produced MWCNTs had diameters ranging from 8 to 34 nm, wall thicknesses of 3-29 nm, and were constructed by 9-85 graphene layers. It is widely accepted that two growth mechanisms exist for CNT formation: (a) tip-growth model, and (b) base-growth model. When the catalyst-substrate interaction is weak (metal has an acute contact angle with the substrate), hydrocarbon decomposes on the top surface of the metal, carbon diffuses down through the metal, and CNT precipitates out across the metal bottom pushing the whole metal particle off the substrate. This is known as "tip-growth model" [12]. In the other case, when the catalyst-substrate interaction is strong (metal has an obtuse contact angle with the substrate), initial hydrocarbon decomposition and carbon diffusion take place similar to those in the tip-growth case, but the CNT precipitation fails to push the metal particle up; thus, the precipitation is compelled to emerge out from the metal's apex (farthest from the substrate, having minimum interaction with the substrate). First, carbon crystallizes out as a hemispherical dome, which then extends up in the form of seamless graphitic cylinder. Subsequent hydrocarbon deposition takes place on the lower peripheral surface of the metal as dissolved carbon diffuses upward. Thus, CNT grows up with the catalyst particle rooted in its base; hence, this is known as "base-growth model" [12]. The red arrows in Figure 6(c) and (d) show the presence of catalyst particles at the tips of CNTs, indicating the "tip-growth model". The darker part in Figure 6(d), shown by black arrow, is a catalytic nanoparticle that was stuck inside carbon nanotube.

Figure 7 represents the Raman spectra of grown CNTs on different (a) C1, (b) C2, (c) C3, (d) C4, and (e) C5 catalyst samples. The Raman band appearing in 1500-1605 cm^{-1} region of the wave number is attributed to G band (graphite band) and the one appearing in 1250-1450 cm^{-1} spectral region is known as D band (disorder-induced band) [22]. The G and D bands are characteristic of sp^2-carbon systems: the G vibration is due to the in-plane bond stretching motion of carbon pairs whereas the D one is a breathing mode

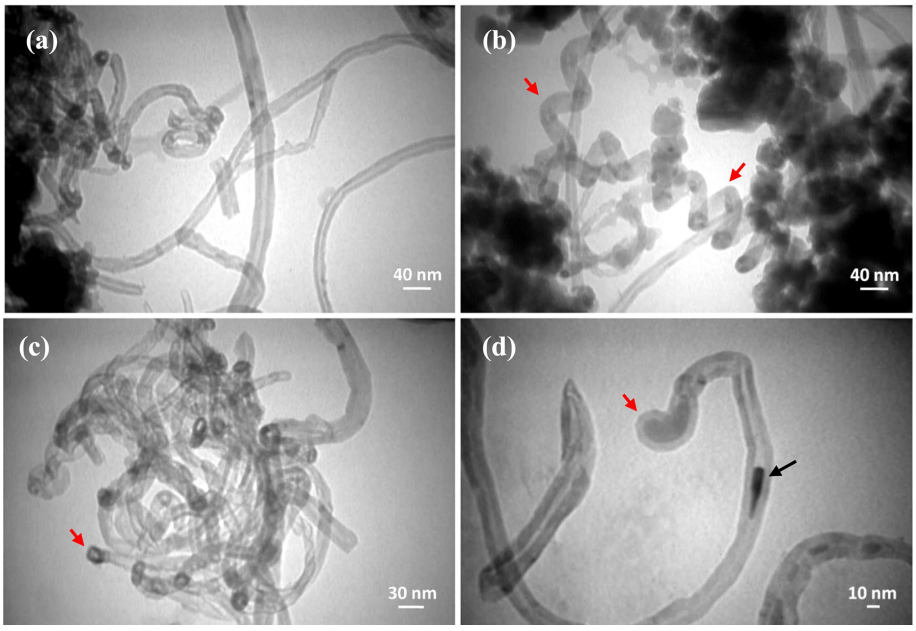

Figure 6. TEM images of CNTs synthesized on C3 catalyst sample.

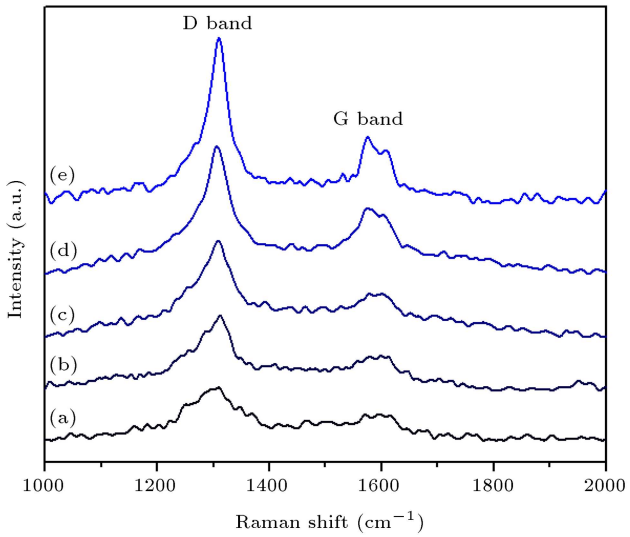

Figure 7. Raman spectra of grown CNTs on (a) C1, (b) C2, (c) C3, (d) C4, and (e) C5 catalyst samples.

Table 4. Raman I_G/I_D ratio of the synthesized CNTs on different catalyst samples.

Catalyst	I_G/I_D of grown CNT
C1	0.49
C2	0.46
C3	0.47
C4	0.52
C5	0.40

of six fold rings and becomes active only in disordered systems [23]. The intensity ratio of G-band to D-band, I_G/I_D, indicates the quality and crystallinity of the produced CNTs, which are exhibited in Table 4. Excluding the one obtained on pure Co catalyst (sample C5), the CNTs grown on different catalysts with different metal loadings have roughly similar qualities. In other words, they have approximately the same level of defects. The worst quality of CNTs on sample C5 is expected to be due to the poor activity of monometallic Co catalyst on SiC substrate.

4. Conclusions

MWCNTs were synthesized by thermal decomposition of acetylene over bimetallic Fe-Co catalysts supported on nanometric SiC and the effect of Fe:Co loading proportion on characteristics of the produced CNTs was investigated. The results showed that bimetallic Fe-Co catalyst with 10:10 wt% was more active than other catalyst compositions and the CNTs nucleated from this sample possessed the smallest average diameter. It was observed that iron oxide nanoparticles had very higher efficiency for CNT production on nanometric SiC support than cobalt oxide particles.

References

1. Eatemadi, A., Daraee, H., Karimkhanloo, H., Kouhi, M., Zarghami, N., Akbarzadeh, A. and Joo, S.W. "Carbon nanotubes: Properties, synthesis, purification, and medical applications", *Nanoscale Res. Lett.*, **9**(1), pp. 1-13 (2014).
2. Purohit, R., Purohit, K., Rana, S., Rana, R.S. and Patel, V. "Carbon nanotubes and their growth methods", *Procedia Mater. Sci.*, **6**, pp. 716-728 (2014).
3. Arora, N. and Sharma, N.N. "Arc discharge synthesis of carbon nanotubes: Comprehensive review", *Diam. Relat. Mater.*, **50**, pp. 135-150 (2014).
4. Tripathi, G., Tripathi, B., Sharma, M.K., Vijay, Y.K., Chandra, A. and Jain, I.P. "A comparative study of arc discharge and chemical vapor deposition synthesized carbon nanotubes", *Int. J. Hydrogen Energy*, **37**(4), pp. 3833-3838 (2012).
5. Berkmans, A.J., Ramakrishnan, S., Jain, G. and Haridoss, P. "Aligning carbon nanotubes, synthesized using the arc discharge technique, during and after synthesis", *Carbon*, **55**, pp. 185-195 (2013).
6. Chrzanowska, J., Hoffman, J., Malolepszy, A., Mazurkiewicz, M., Kowalewski, T.A., Szymanski, Z. and Stobinski, L. "Synthesis of carbon nanotubes by the laser ablation method: Effect of laser wavelength", *Phys. Status Solidi B*, **252**(8), pp. 1860-1867 (2015).
7. Jiang, W., Molian, P. and Ferkel, H. "Rapid production of carbon nanotubes by high-power laser ablation", *J. Manuf. Sci. E.*, **127**(3), pp. 703-707 (2005).
8. Shah, K.A. and Tali, B.A. "Synthesis of carbon nanotubes by catalytic chemical vapour deposition: A review on carbon sources, catalysts and substrates", *Mat. Sci. Semicon. Proc.*, **41**, pp. 67-82 (2016).
9. Lobiak, E.V., Shlyakhova, E.V., Bulusheva, L.G., Plyusnin, P.E., Shubin, Y.V. and Okotrub, A.V. "Ni-Mo and Co-Mo alloy nanoparticles for catalytic chemical vapor deposition synthesis of carbon nanotubes", *J. Alloy. Compd.*, **621**, pp. 351-356 (2015).
10. Gulino, G., Vieira, R., Amadou, J., Nguyen, P., Ledoux, M.J., Galvagno, S. and Pham-Huu, C. "C_2H_6 as an active carbon source for a large scale synthesis of carbon nanotubes by chemical vapour deposition", *Appl. Catal. A-gen.*, **279**(1), pp. 89-97 (2005).
11. Takagi, D., Hibino, H., Suzuki, S., Kobayashi, Y. and Homma, Y. "Carbon nanotube growth from semiconductor nanoparticles", *Nano Lett.*, **7**(8), pp. 2272-2275 (2007).
12. Kumar, M. and Ando, Y. "Chemical vapor deposition of carbon nanotubes: a review on growth mechanism and mass production", *J. Nanosci. Nanotechnol.*, **10**(6), pp. 3739-3758 (2010).
13. De Volder, M.F.L., Tawfick, S.H., Baughman, R.H. and Hart, A.J. "Carbon nanotubes: Present and future commercial applications", *Science*, **339**, pp. 535-539 (2013).

14. Hu, X., Cook, S., Wang, P., Hwang, H.M., Liu, X. and Williams, Q.L. "In vitro evaluation of cytotoxicity of engineered carbon nanotubes in selected human cell lines", *Sci. Total Environ.*, **408**(8), pp. 1812-1817 (2010).

15. Baughman, R.H., Zakhidov, A.A. and de Heer, W.A. "Carbon nanotubes-the route toward applications", *Science*, **297**(5582), pp. 787-792 (2002).

16. Ci, L., Ryu, Z., Jin-Phillipp, N.Y. and Rühle, M. "Carbon nanotubes/SiC whiskers composite prepared by CVD method", *Diam. Relat. Mater.*, **16**(3), pp. 531-536 (2007).

17. Murakami, T., Sako, T., Harima, H., Kisoda, K., Mitikami, K. and Isshiki, T. "Raman study of SWNTs grown by CCVD method on SiC", *Thin Solid Films*, **464**, pp. 319-322 (2004).

18. Khorsand Zak, A., Majid, W.H.A., Ebrahimizadeh Abrishami, M., Yousefi, R. and Parvizi, R. "Synthesis, magnetic properties and X-ray analysis of Zn0.97X0.03O nanoparticles(X=Mn, Ni, and Co) using Scherrer and size-strain plot methods", *Solid State Sci.*, **14**, pp. 488-494 (2012).

19. Dupuis, A.C. "The catalyst in the CCVD of carbon nanotubes-a review", *Prog. Mater. Sci.*, **50**(8), pp. 929-961 (2005).

20. Klinke, C., Bonard, J.M. and Kern, K. "Comparative study of the catalytic growth of patterned carbon nanotube films", *Surf. Sci.*, **492**(1), pp. 195-201 (2001).

21. Hernadi, K., Fonseca, A., Nagy, J.B., Siska, A. and Kiricsi, I. "Production of nanotubes by the catalytic decomposition of different carbon-containing compounds", *Appl. Catal. A-gen.*, **199**(2), pp. 245-255 (2000).

22. Dresselhaus, M.S., Dresselhaus, G., Saito, R. and Jorio, A. "Raman spectroscopy of carbon nanotubes", *Phys. Rep.*, **409**(2), pp. 47-99 (2005).

23. Botti, S., Ciardi, R., Asilyan, L., De Dominicis, L., Fabbri, F., Orlanducci, S. and Fiori, A. "Carbon nanotubes grown by laser-annealing of SiC nanoparticles", *Chem. Phys. Lett.*, **400**(1), pp. 264-267 (2004).

Biographies

Fatemeh Shahi received her BSc degree from Behshar Payame Noor University and MSc degree (ranked first) from University of Mazandaran (Solid State Physics) in 2014. She is currently a physics teacher at non-governmental and non-profit higher education institute of Andisheh sazan e Neka; also, she is preparing for PhD entrance test. Her research interests include the synthesis and applications of carbon nanotubes.

Mohammad Akbarzadeh Pasha received his BSc degree in the Faculty of Basic Science (Solid State Physics) from University of Mazandaran and his MSc and PhD degrees in the Faculty of Physics (Condensed Mater Physics) from Sharif University of Technology, Iran. From July 2012, he has worked as an Assistant Professor in the Faculty of Basic Science at University of Mazandaran and since 2014 he has been the Head of the research lab of Carbon based nanostructures in that university. During 2014-2015, he was the Head of Department of Solid State Physics at University of Mazandaran. His research interests include the synthesis of carbon nanotubes (CNTs), transition metal catalyst nanoparticles, and CNT-inorganic hybrids and their applications.